Original Research

CARDIOLOGY

Cardiology 2015;132:111–118
DOI: 10.1159/000431283

Received: January 29, 2015
Accepted after revision: May 8, 2015
Published online: July 1, 2015

Comparison of Left Ventricular Myocardial Structure and Function in Patients with Aortic Stenosis and Those with Pure Aortic Regurgitation

Vito Mannacio[a] Elia Guadagno[b] Luigi Mannacio[a] Mariarosaria Cervasio[b]
Anita Antignano[d] Michele Mottola[a] Cesare Gagliardi[c] Carlo Vosa[a]

Departments of [a]Cardiac Surgery, [b]Advanced Biosciences and [c]Public Health, University Federico II School of Medicine, and [d]Department of Cardiology, Azienda Ospedaliera Santobono-Pausillipon, Naples, Italy

Key Words
Aortic valve replacement · Aortic stenosis · Aortic regurgitation · Cardiomyocytes · Left ventricular function

Abstract
Objective: We aimed to support the structural and functional distinction between aortic stenosis (AS) and aortic regurgitation (AR). ***Methods:*** Biopsy specimens taken from 70 selected patients (35 with AS and 35 with AR) undergoing aortic valve replacement (AVR) were analyzed for their cardiomyocyte dimensions and structure, interstitial fibrosis and contractile function. To determine normal values of contractile function, 10 donor hearts were analyzed. ***Results:*** Cardiomyocyte diameter was higher in AS than in AR (22.7 ± 2.2 vs. 13.2 ± 0.7 μm, $p < 0.001$). Length was higher in AR (121.2 ± 9.4 vs. 95.6 ± 3.7 μm, $p < 0.001$). Collagen volume fraction was increased in both AS and AR, but was lower in the AS specimens (7.7 ± 2.3 vs. 8.9 ± 2.3, $p = 0.01$). Myofibril density was reduced in AR (38 ± 4 vs. 48 ± 5%, $p < 0.001$). Cardiomyocyte diameter and length were closely linked to the relative left ventricular (LV) wall thickness ($R^2 = 0.85$, $p < 0.001$ and $R^2 = 0.68$, $p = 0.003$). The cardiomyocytes of AS patients had higher $F_{passive}$ (6.6 ± 0.3 vs. 4.6 ± 0.2 kN/m^2, $p < 0.001$), but their total force was comparable. $F_{passive}$ was also significantly higher in AS patients with restrictive rather than pseudo-normal LV filling (7.3 ± 0.5 vs. 6.7 ± 0.6, $p = 0.004$). In AS patients, but not in AR patients, $F_{passive}$ showed a significant association with the cardiomyocyte diameter ($R^2 = 0.88$, $p < 0.001$ vs. $R^2 = 0.31$, $p = 0.6$). ***Conclusions:*** LV myocardial structure and function differ in AS and AR, allowing for compensative adjustment of the diastolic/systolic properties of the myocardium.

Introduction

Aortic stenosis (AS) and aortic regurgitation (AR) have their own physiology, anatomy, histology and clinical outcome. The pathophysiology of pure AS is mainly characterized by pressure overload; in AR, volume overload is the main compensative mechanism [1]. Pressure and volume overload lead to structural modifications which contribute to the functional changes of the heart. Different adaptations consist of myocardial stiffness and diastolic or systolic dysfunction which reflect specific cardiomyocyte remodeling and the derangement of intersti-

E-Mail karger@karger.com
www.karger.com/crd

Vito Mannacio
Via S. Domenico 62
IT–80127 Naples (Italy)
E-Mail vitomannacio2@libero.it

Table 1. Clinical profile of patients

	AS (n = 35)	AR (n = 35)	p
Age, years (mean ± SD)	62±7	60±6	0.3
Female gender, n	12 (34%)	15 (43%)	0.8
Body mass index (mean ± SD)	24±4	25±4	0.2
Hypertension, n	15 (43%)	18 (51%)	0.6

Hypertension was considered as a blood pressure >140/90 mm Hg.

tial collagen and elastic compounds [2–5]. However, despite many studies having been published, some aspects of the relationships between structure and function in AS and in AR have not been definitively assessed. Mechanobiological research is hampered because of the difficulty collecting human specimens in vivo, and studies on animal models or on in vitro cultured cells do not, effectively, display human-like behavior. We analyzed the left ventricle biopsy samples obtained from patients with AS and AR during surgery for aortic valve replacement (AVR), in order to evaluate cellular morphology, interstitial fibrosis and force measurements in isolated cardiomyocytes. The results were correlated with left-ventricular (LV) geometry determined by echocardiography. A group of normal donor hearts was also analyzed as controls for the histological analysis.

Materials and Method

This study was designed according to the Standards for Reporting of Diagnostic Accuracy.

The study population consisted of 70 patients (35 with pure AS and 35 with pure AR) who underwent primary isolated AVR between September 2012 and May 2014. According to the ACC/AHA 2006 guidelines, indications for AVR in patients with AS are: area <1.0 cm^2, mean gradient >40 mm Hg, jet velocity >4.0 m/s in symptomatic patients, and area <0.6 cm^2, mean gradient >60 mm Hg, jet velocity >5.0 m/s in asymptomatic patients. The indications for AVR in patients with AR were: LV dysfunction, i.e. LV ejection fraction (LVEF) ≤0.50 in symptomatic or asymptomatic patients, and normal LV systolic function, i.e. LVEF >0.50 but with severe LV dilatation (end-diastolic dimension >75 mm or end-systolic dimension >55 mm) in asymptomatic patients [6].

The general exclusion criteria were: severe comorbidities (e.g. dialysis or hepatic failure), autoimmune diseases (systemic lupus erythematosus, rheumatoid arthritis, scleroderma, Sjögren's syndrome or psoriatic arthritis) or connective tissue disorders (Marfan syndrome, Ehlers-Danlos syndrome or Loeys-Dietz syndrome), acute aortic dissection, congenital defects of the aortic valve (bicuspid valve or subvalvular stenosis induced by fixed or dynamic components), atrial fibrillation, contemporary mitral and/or tricuspid valve stenosis or regurgitation, evidence of coronary stenosis and active endocarditis. We considered only negligible regurgitation (in AS patients) or stenosis (in AR patients) to be tolerable. The etiology of AS was degenerative (senility, wear and tear, calcification and atherosclerosis) in 23 cases, rheumatic in 6 and indeterminate in 6. The etiology of AR was rheumatic in 22 cases, a chronic consequence of previous bacterial endocarditis in 6, degenerative (idiopathic annuloaortic ectasia or floppy aortic valve) in 5 and indeterminate in 2. To avoid the bias due to different age distribution in the groups, we included only patients who were 50–70 years old. There was echocardiographic evidence of pressure overload in all AS patients and of volume overload in all AR patients. Patients with diabetes mellitus were excluded due to possible collagen derangements that could hinder the correct evaluation of the interstitial fibrosis. A further exclusion criterion in patients with AS was a reduced LV systolic function, i.e. LVEF <0.50. All patients underwent preoperative conventional coronary angiography or 64-slice multidetector computed tomography [7].

Ten normal hearts obtained from donors for transplantation were analyzed as controls. Their age range was 17–42 years (mean 28.7 ± 7.1). These controls had normal cardiac dimensions, wall thickness and LVEF. The main clinical and demographic characteristics of the study cohort are reported in table 1. All patients provided written informed consent prior the inclusion and the Institutional Research Ethics Committee approved the study.

Echocardiographic Measurements and Calculations

Transthoracic examination was performed in all patients. When it was considered inadequate, the transesophageal approach was employed. AS was graded according to EAE/ASE recommendations and AR according to ASE recommendations [8, 9]. Size, geometry and function were evaluated according to ESC recommendations [10]. Peak and mean aortic gradients were calculated from continuous-wave Doppler by the modified Bernoulli equation and the aortic valve area with the continuity equation. The LV function was evaluated as LVEF calculated by the Simpson rule and the endocardial and mid-wall fractional shortening. The LV mass index (LVMI) was calculated from LV linear dimensions by the ASE-recommended formula and was normalized to body surface area. Calculation of relative wall thickness permitted categorization of LV hypertrophy as concentric (≥0.42) or eccentric (≤0.42). Patterns of LV remodeling were classified following the scheme proposed by Gaasch and Zile [11]. Pulse-wave tissue Doppler imaging was performed in the apical views to acquire mitral annular velocities and support 2-dimensional images for LV diastolic analysis.

Table 2. Echocardiographic LV morphologic and functional characteristics

	AS (n = 35)	AR (n = 35)
LV end-diastolic volume, ml/m^2	70±8	115±29
LV peak systolic volume, ml/m^2	21±4	55.3±7.3
LVEF, %	67±5	51±6
LVMI, g/m^2	144±12	212±29
LV mass/volume ratio	1.2±0.2	0.9±0.05
Relative wall thickness, %	0.5±0.04	0.3±0.03
LV posterior wall thickness in the diastole, mm	12±2	11±2
Interventricular septum thickness in the diastole, mm	13±1	12±2
Indexed left-atrium diameter, mm/m^2	25±2	22±2
Pulmonary artery systolic pressure, mm Hg	61±7	30±8
Indexed aortic valve area, cm^2/m^2	0.6±0.03	
Peak velocity, m/s	4±0.04	
Peak transvalvular gradient	108±18	
Mean transvalvular gradient	59±7	
Deceleration time, m/s	164±25	
Diastolic flow reversal		prominent holodiastolic
Regurgitant jet/left ventricle outflow tract width, %[a]		0.6±0.07
Vena contracta width, cm[a]		0.6±0.02
Regurgitant volume, ml/beat		57±5
Regurgitant fraction, %		54±6
Effective regurgitant orifice area, cm^2		30±4
Endocardial fractional shortening, %	28±2	20±3
Mid-wall fractional shortening, %	21±2	13±3

Values are mean ± SD.
[a] At a Nyquist limit of 50–60 cm/s.

Myocardial Biopsies

Full-thickness specimens from the apex of the left ventricle were obtained before cannulation for cardiopulmonary bypass to avoid interferences due to handling, hypothermia or cardioplegia. All donor hearts were sampled from the apex just before being explanted. Six donor hearts were additionally sampled from the LV mid-lateral wall to evaluate the difference between the apex and the lateral LV wall. Biopsy products were divided into samples of about 5–8 mg each. Three were fixed in 5% formalin at room temperature and 3–4 were analyzed within 1–3 h for cardiomyocyte force measurements. The formalin-fixed biopsies were used for histomorphometry. Histologic evaluation was performed by 2 pathologists blinded to the condition of the patients.

Light Microscopy

Light microscopy was performed for cardiomyocyte dimensions on 4-μm-thick sections of formalin-fixed tissue stained with hematoxylin and eosin (HE). Histochemical staining (i.e. Picrosirius red, Masson trichrome and Van Gieson) techniques were used for the tissue components. Areas of reparative and perivascular fibrosis were excluded.

When mechanical disruption of the tissue structure was seen, the biopsy sample was excluded. Subsequent image analysis with Scion Image 4.0.3.2 software (Scion Corporation, Frederick, Md., USA) was performed to determine cardiomyocyte diameter (MyD) and length (MyL) in micrometers as well as the extent of interstitial fibrosis. MyD perpendicular to the outer contour of the cell membrane at the nucleus region and MyL as the distance between intercalated disks were determined in at least 10 myocytes after the exclusion of clearly transverse or oblique-cut myocytes. Interstitial fibrosis was measured as the percentage of connective areas averaged over 5 representative fields and expressed as connective volume fraction (CVF). Based on CVF values, the extent of interstitial fibrosis was graded as low (0–5%, class I), intermediate (5–10%, class II), or high (10–15%, class III) [2].

Electron Microscopy

Biopsy samples were fixed in 2.5% glutaraldehyde/0.1 M cacodylate buffer, rinsed in cacodylate buffer, fixed in 1% osmium tetroxyde/0.1 M cacodylate buffer, and then rinsed again in buffer. Tissue samples were gradually dehydrated in a series of ascending concentrations of ethanol, and then immersed in propylene oxide before infiltration with the epoxy resin Epon 812. Ultrathin sections were collected on 100-mesh copper grids and double-stained with uranyl acetate and lead citrate. Sections were examined in a Zeiss 900 transmission.

Cardiomyocyte myofibrillar density and the number of mitochondria were determined. Myofibrillar density was estimated as the proportion of the sum of myofibrillar areas related to total cellular area in 5–8 representative myocytes, and recorded as myofibril volume fraction (MVF).

Force Measurements in Isolated Cardiomyocytes

Force measurements were performed in single, mechanically isolated cardiomyocytes following the protocol described by Falcão-Pires et al. [12] and Borbély et al. [13]. Biopsy samples (4–5 mg wet weight) were defrosted, dissected into strips and placed in a skinning solution (all in mM: free Mg 1, KCl 100, ethylene glycol tetraacetic acid 2, Mg-ATP 4 and imidazole 10; pH 7.0) and mechanically minced. To remove all membrane residuals, samples were incubated for 5 min in relaxing solution supplemented with 0.2% Triton X-100, in order to obtain cardiomyocytes dependent only on externally supplied calcium for force development. Single myocytes were suspended between a force transducer and a piezoelectric actuator. First-order laser diffraction was used to determine sarcomere length, which was held constant at 2.2 μm. Myocytes were relaxed and activated at various Ca^{2+} concentrations [$pCa = -10\log(Ca^{2+})$]. The solution contained 1,2-bis(2-aminophenoxy) ethane-N,N,N′N′-tetraacetic acid as a Ca^{2+} buffer. Starting from pCa 9.0 m (relaxation), exposed to a series of solutions, maximal activation was obtained at pCa 4.5. The maximal activation was used to calculate maximal calcium-activated isometric force (F_{max}). Once a steady-state force level was reached, the length of the myocyte was reduced by 20% within 2 ms by means of the piezoelectric motor (slack test). The distance between the baseline and the steady-state force level was the total force (F_{total}). The cell was then restretched and returned to the relaxing solution, in which a second slack test of 10-second duration was performed to determine the pas-

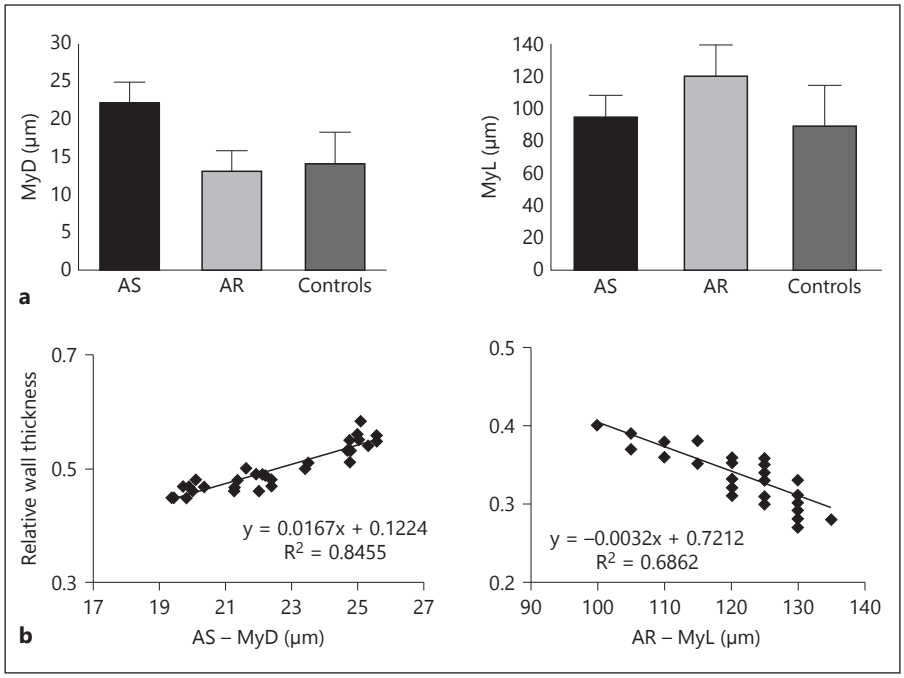

Fig. 1. a Bar graph display of cardiomyocytes dimension in the left ventricles of patients with AS or AR compared to controls. **b** Cardiomyocyte dimensions analyzed for correlation to concentric (RWT ≥0.42) or eccentric (RWT ≤0.42) hypertrophy.

sive force ($F_{passive}$). Maximal calcium activated tension (F_{active}) was calculated by subtracting $F_{passive}$ from F_{total} at saturating Ca^{2+} (pCa 4.5).

Statistics

Values are given as mean ± SD. The Mann-Whitney U test was used for variables not normally distributed. Categorical variables were analyzed with the χ^2 test or the Fisher exact test when appropriate. The Pearson correlation coefficient was used to assess the association between variables. In addition, pairwise correlations were determined by linear regression analysis. A p value of <0.05 was considered significant. Data were analyzed by SPSS version 15 for Windows (SPSS, Inc., Chicago, Ill., USA).

Results

Echocardiography

Preoperative echocardiographic characteristics are summarized in table 2. Regarding AR, quantitative parameters should be viewed with caution and only in the context of the other signs of severity because of the intrinsic limitations of quantitative measurement techniques. All patients had an increased LVMI. In the AS patients, grade II LV diastolic dysfunction (pseudo-normal filling of the left ventricle) occurred in 25 patients (71.4%) and grade III (restrictive filling of the left ventricle) in 10 (28.6%). All AR patients had LV dilatation. Eight patients (22.8%) showed preserved LV function, 16 (45.7%) had an LVEF of 40–50%, 6 (17.2%) of 30–40% and 5 (14.3%) of <30%. According to the scheme of LV remodeling based on volume, mass and geometry, all of the AS patients had concentric hypertrophy; 8 of the AR patients (26.6%) had physiologic hypertrophy and 22 (73.4%) had eccentric hypertrophy.

Morphometric Analysis

In the donor hearts, MyD, MyL, CVF and MVF were 14 ± 2 μm, 90 ± 15 μm, 5 ± 2% and 50 ± 4%, respectively. No significant differences were detected between the apex and mid-lateral LV wall. The MyD was significantly increased in the AS hearts (22.5 ± 2.2 μm, $p < 0.001$), but the MyL (95.6 ± 3.7 μm, $p = 0.1$) remained unchanged. In the AR hearts, there were few/no changes in the MyD (13.2 ± 0.7 μm, $p = 0.1$), but the MyL was significantly greater (121.1 ± 8.4 μm, $p < 0.001$; fig. 1a). The MyD was in close linear relation to the degree of concentric hypertrophy ($R^2 = 0.84$, $p < 0.001$) and the MyL with the degree of eccentric hypertrophy ($R^2 = 0.68$, $p = 0.008$; fig. 1b). Myofibrillar density, evaluated as MVF, was significantly lower in AR patients than in AS patients (38 ± 4 vs. 49 ± 5%, $p < 0.001$). The basic structure of sarcomeres was preserved in both groups. The MVF and MyD were in close linear relation in both the AS ($R^2 = 0.76$, $p = 0.002$) and AR ($R^2 = 0.79$, $p = 0.001$) specimens. The higher degree of LV diastolic dysfunction in AS patients tended to relate

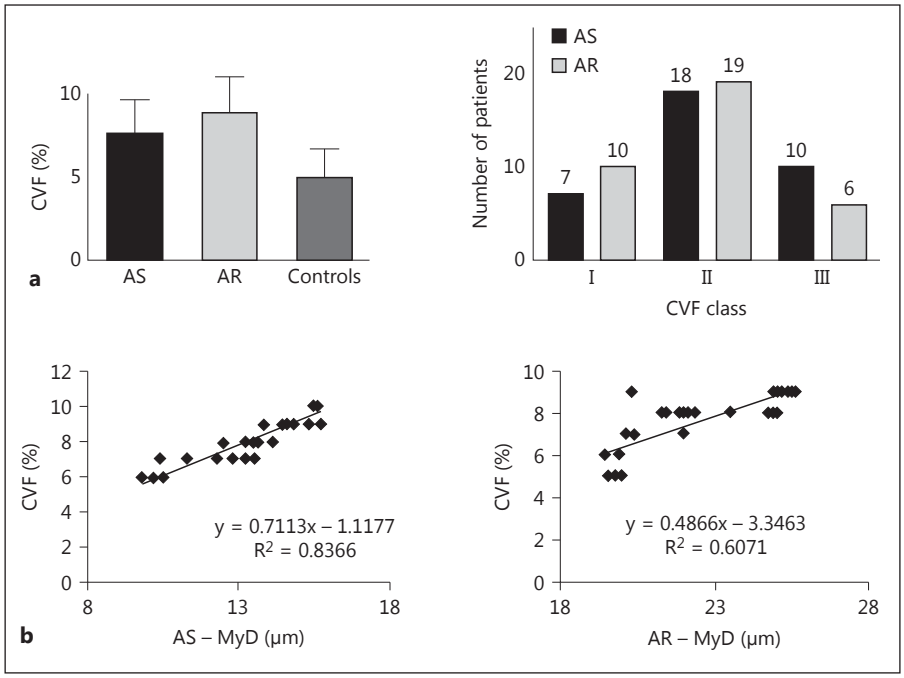

Fig. 2. a Bar graph display of CVF in the specimens of patients with aortic stenosis or aortic regurgitation compared to controls and of distribution of patients with low (I class), intermediate (II class) or high (III class) CVF. Numbers over bars indicate individuals in each group. **b** Cardiomyocyte dimensions analyzed for correlation to CVF in the specimens of patients with AS or AR.

to the higher MVF ($R^2 = 0.61$, $p = 0.04$) and MyD ($R^2 = 0.52$, $p = 0.05$). The higher LV diastolic volume in AR patients tended to relate to the higher MyL ($R^2 = 0.66$, $p = 0.4$) but not to the MVF ($R^2 = 0.4$, $p = 0.08$). In the AS specimens, the sarcomere width was increased as a possible consequence of its parallel replication; in AR specimens, it was reduced as it was replicated mainly in series.

Compared to normal values, the interstitial fibrosis was significantly increased in both the AS and AR specimens ($p < 0.001$). However, AS patients had a higher CVF than AR patients (8.9 ± 2.3 vs. 7.7 ± 2.3, $p = 0.01$) and there was a different distribution of low, intermediate or high CVF in the AS and AR samples (fig. 2a). The CVF and MyD showed a positive linear correlation in both AS ($R^2 = 0.83$, $p = 0.003$) and AR ($R^2 = 0.61$, $p = 0.01$) specimens (fig. 2b). Notably, AS specimens revealed a high degree of disarray of interstitial connective fibers. Collagen deposits interrupted the normal juxtaposition of cardiomyocytes in the AS samples, but were normally distributed in AR specimens (fig. 3a: a3, a4 and b2, b3).

In the control myocytes, the number and the size of mitochondria were 30–40% of total volume and 0.5–1 × 3–5 μm, respectively. They were unmodified in the AS samples but were increased in the AR myocytes (40–45% of myocyte volume and 0.7–1.2 × 5–7 μm). In the AR myocytes, mitochondria were not only positioned outside the myofibrils (as in normal or in AS myocytes) but also inside them (fig. 3b: a3 and b1–3). Ultrastructural images were observed in AS myocytes, but not in AR myocytes, in the areas of vacuolization and in the lipofuscin granules adjacent to the nucleus and interposed inside the myofibrils (fig. 3a: a1, a2; fig. 3b: a1, a2). Furthermore, interruption of subendocardial elastic-fiber network was found in AR specimens but not in AS specimens (fig. 3a: a4, b4).

Measurement of Mechanical Properties

In the donor hearts, $F_{passive}$ and F_{total} at a maximal activation of cardiomyocytes were 3.6 ± 0.4 and 21.2 ± 3.1 kN/m^2, respectively. The average force-pCa relations are shown in figure 4a. F_{total} at pCa 4.5 was similar in AS and AR myocytes (19.5 ± 5.2 vs. 18.5 ± 8.3 kN/m^2, $p = 0.5$).

$F_{passive}$ was higher in AS than in AR (6.6 ± 0.3 vs. 4.6 ± 0.2 kN/m^2, $p < 0.001$; fig. 4b). In AS patients, the higher $F_{passive}$, evaluated by means of linear regression analysis, showed a close relationship with the higher cardiomyocyte diameter ($R^2 = 0.88$, $p < 0.001$), but in AR patients, there was no similar relationship with the increased cardiomyocyte length ($R^2 = 0.25$, $p = 0.7$). Consequently, $F_{passive}$ was significantly higher in AS patients with grade III (restrictive filling) rather than with grade II (pseudo-normal filling) LV diastolic dysfunction (7.3 ± 0.5 vs. 6.7 ± 0.6, $p = 0.004$). $F_{passive}$ was, moreover, independent of the LVEF ($p = 0.7$), the peak LV systolic volume ($p = 0.6$) and the end LV diastolic volume ($p = 0.7$).

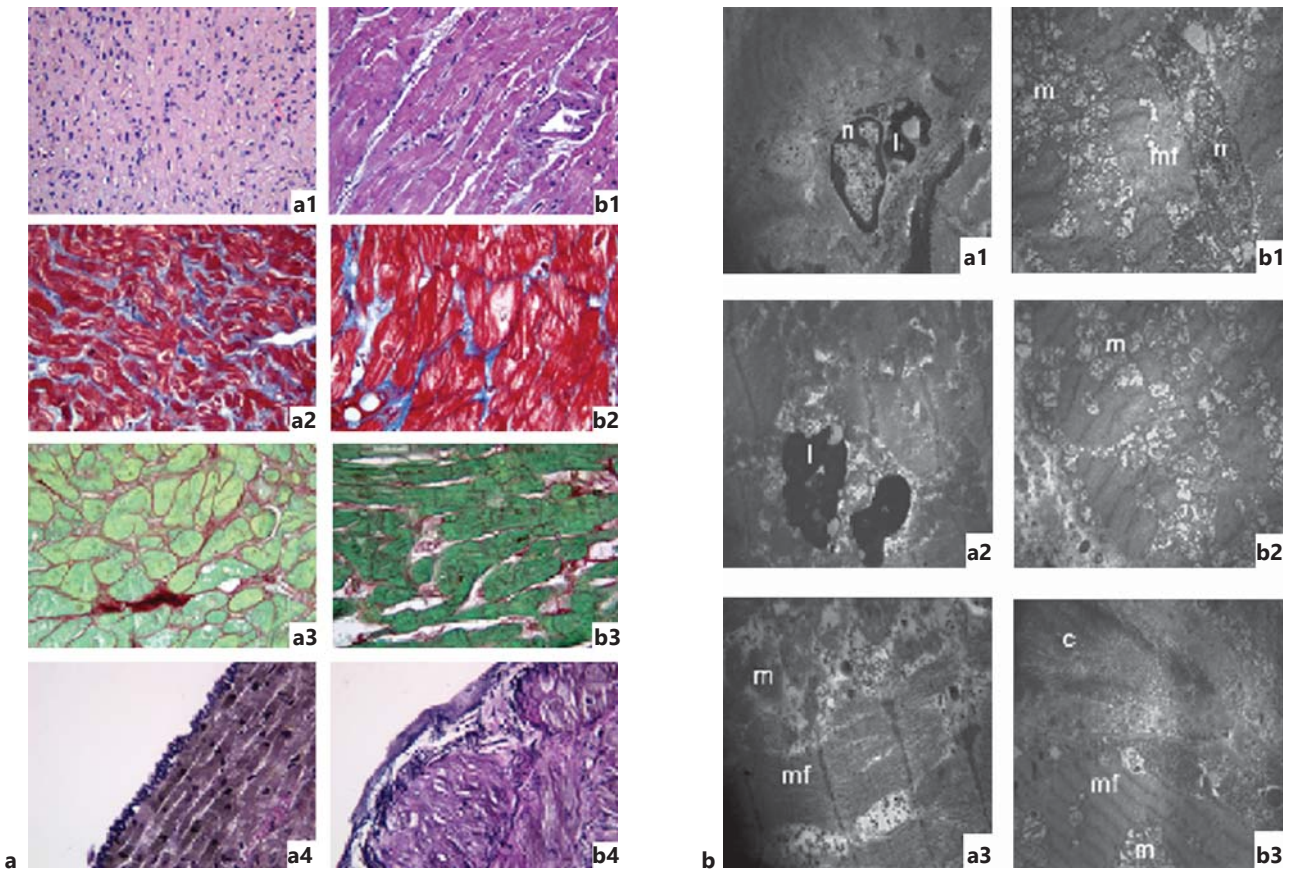

Color version available online

Fig. 3. a Histological images. AS (left column): a1 high cellularity and a large amount of cytoplasmic deposits of lipofuscin (HE, ×40); a2 interstitial fibrosis is more evident (blue) among myocardial tissue (red; Masson trichrome); a3 collagen deposits (red) interrupting normal juxtaposition of cardiomyocytes (green; Picrosirius red); a4 normal network of subendocardial elastic fibers (van Gieson). AR (right column): b1 myocardial disarray (HE, ×40); b2 normal collagen (blue) distribution (Masson trichrome); b3 normal collagen distribution (red) among cardiomyocytes (Picrosirius red); b4 interruption of subendocardial elastic fiber network (van Gieson). **b** Ultrastrucural images obtained by electron microscopy. AS (left column): a1 lipofuscin granules adjacent to the nucleus of myocardiocytes (×3,000); a2 lipofuscin granules interposed between the myofibrils (×4,400); a3 longitudinal section of parallel myofibrils and large mitochondria (×7,000). AR (right column): b1 numerous mitochondria interposed between the myofibrils around the nucleus (×3,000); b2 higher magnification of numerous mitochondria located between the myofibrils (×4,400); b3 numerous collagen fibrils and myofibrils with large mitochondria interposed (×3,000). c = Collagen fibrils; l = lipofuscin granules; m = mitochondria; mf = myofibrils; n = nucleus. (Colors refer to the online version only.)

Discussion

This study yielded the following information: (1) MyD was larger in AS, but MyL was increased in AR, (2) myocardial fibrosis was increased in both AS and AR, but AS patients had a higher CVF than AR patients, (3) myofibril density was higher in AS, reflecting a different sarcomere architectural pattern, (4) the number, size and distribution of mitochondria were increased in AR cardiomyocytes, (5) lipofuscin deposition occurred adjacent to the nucleus and between the myofibrils in the AS samples, (6) at a sarcomere length of 2.2 μm, F_{total} at maximal Ca^{2+} was comparable between AS and AR samples, but $F_{passive}$ was higher in the cardiomyocytes from the AS patients and (7) the structural and functional changes and the difference in systolic and diastolic properties of the left ventricle were in close correlation.

Adults with AS or AR show different functional and geometrical patterns, occurring as adaptive responses to pressure (concentric LV hypertrophy) or volume (ec-

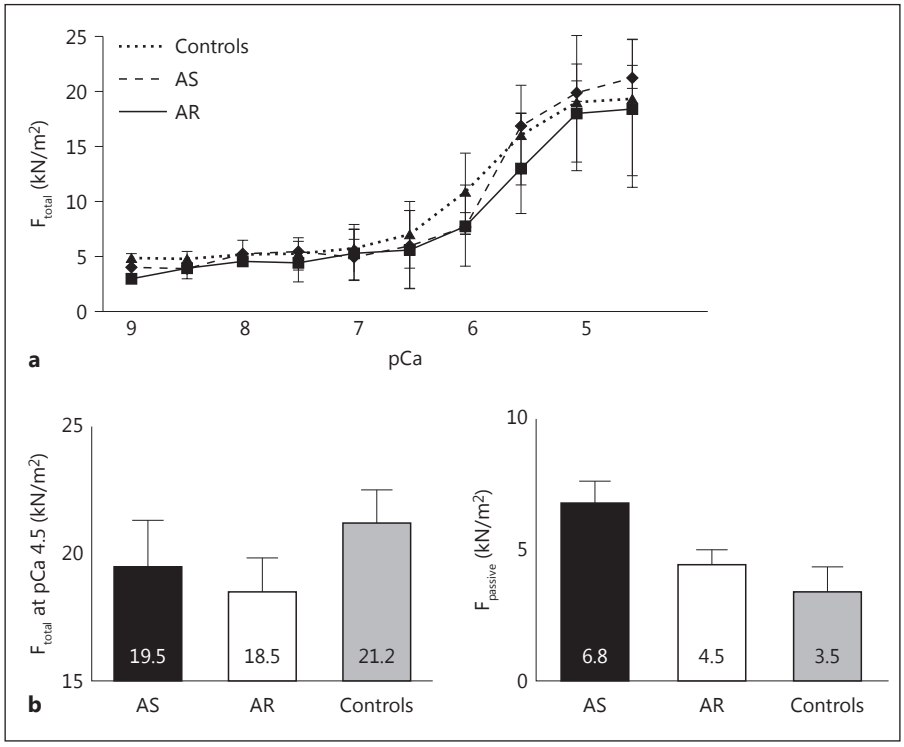

Fig. 4. a Average F_{total}-pCa relation for pooled cardiomyocytes of control, AS and AR groups. **b** Bare graph display of F_{total} at maximal activation and $F_{passive}$ in cardiomyocytes from AS and AR hearts compared to controls.

centric LV hypertrophy) overload [14–16]. The histology is characterized by distinct cardiomyocyte reshaping and interstitial fibrosis [15]. In AS, we observed cardiomyocytes growing in a transverse direction, but the cell length remained almost constant; in AR, they mainly grew in length [16]. The different remodeling reflected different myofibril proportions and sarcomere reshaping. The sarcomeres appeared to be added side-by-side in parallel in AS (where myocardiocytes are wider) and end-to-end in series in AR (where myocardiocytes are longer). These processes are not completely clear, but some studies have suggested that the peak systolic wall stress (pressure overload) or the end-diastolic wall stress (volume overload) could trigger different cell shapes because of distinct growth factors [14]. Reasonably, pressure overload requires wider cardiomyocytes against a greater afterload, and volume overload requires longer cardiomyocytes to modulate the Frank-Starling mechanism.

As a rule, volume and pressure overload require extraordinary energetic support [17–19]. Nonetheless, we observed that the number and size of mitochondria increased only in the AR cardiomyocytes. This appears to be a paradox, considering that AS cardiomyocytes reasonably require higher ATP support. However, it has been reported that, as the demand for ATP increases, levels of phosphocreatine are progressively depleted, and substrate utilization switches toward free fatty acids [20]; this increases the production of reactive oxygen species [17]. Oxidatively damaged mitochondria become the target for phagocytosis, with lysosomes starting the lipofuscinogenesis [21]. Accordingly, we detected granules of lipofuscin in the cardiomyocytes from the AS patients. Finally, we established an interesting correlation between myocyte remodeling and patterns of interstitial fibrosis consistent with the different geometric and functional properties of the left ventricle in AS patients versus AR patients. Furthermore, the analysis of contractile function demonstrated a similar F_{total} but an increased resting tension ($F_{passive}$) in AS patients, both of which likely reflect not only the rearray of myofibrils inside the sarcomere but also a shift toward other isoforms with different functional properties (i.e. β-myosin heavy channel by α-myosin heavy channel, N2BA titin isoform by N2BA isoform and obscurin A by obscurin B) [13, 14, 22–25].

Limitations

The statistical power of this study may have been hampered by the small size of our cohort. All biopsy samples were derived from the apex, so myocardial tissue heterogeneity as a major factor of bias would have been overlooked.

Conclusions

The study demonstrated that the LV myocardium in AS and AR differs in both its cellular architecture and function. These structural and functional abnormalities allow for the compensative adjustment of the diastolic/systolic properties of the myocardium.

Conflict of Interest

There were no conflicts of interest declared.

References

1 Chatterjee K, Massie B: Systolic and diastolic heart failure: differences and similarities. J Cardiac Fail 2007;13:569–576.
2 Borbély A, van der Velden J, Papp Z, Bronzwaer JGF, Edes I, Stienen GJM, Paulus WJ: Cardiomyocyte stiffness in diastolic heart failure. Circulation 2005;111:774–781.
3 Van Heerebeek L, Borbély A, Niessen HWM, Bronzwaer JG, van der Velden J, Stienen GJ, Linke WA, Laarman GJ, Paulus WJ: Myocardial structure and function differ in systolic and diastolic heart failure. Circulation 2006;113:1966–1973.
4 Grossman W, Paulus WJ: Myocardial stress and hypertrophy: a complex interface between biophysics and cardiac remodeling. J Clin Invest 2013;123:3701–3703.
5 Taniguchi K, Kawamaoto T, Kuki S, Masai T, Mitsuno M, Nakano S, Kawashima Y, Matsuda H: Left ventricular myocardial remodeling and contractile state in chronic aortic regurgitation. Clin Cardiol 2000;23:608–614.
6 Bonow RO, Carabello BA, Kanu C, de Leon AC Jr, Faxon DP, Freed MD, Gaasch WH, Lytle BW, Nishimura RA, O'Gara PT, O'Rourke RA, Otto CM, Shah PM, Shanewise JS, Smith SC Jr, Jacobs AK, Adams CD, Anderson JL, Antman EM, Faxon DP, Fuster V, Halperin JL, Hiratzka LF, Hunt SA, Lytle BW, Nishimura R, Page RL, Riegel B: ACC/AHA 2006 guidelines for the management of patients with valvular heart disease. Circulation 2006;114:e84–e231.
7 Mannacio VA, Imbriaco M, Iesu S, Giordano AL, Di Tommaso L, Vosa C: 64-Slice multidetector computed tomographic evaluation of arterial conduit patency after off-pump coronary artery bypass grafting. Tex Heart Inst J 2009;36:409–415.
8 Baumgartner H, Hung J, Bermejo J, Chambers JB, Evangelista A, Griffin BP, Iung B, Otto CM, Pellikka PA, Quiñones M: Echocardiographic assessment of valve stenosis: EAE/ASE recommendations for clinical practice. Eur J Echocardiogr 2009;10:1–25.
9 Zoghbi WA, Enriquez-Sarano M, Foster E, Grayburn PA, Kraft CD, Levine RA, Nihoyannopoulos P, Otto CM, Quinones MA, Rakowski H, Stewart WJ, Waggoner A, Weissman NJ: Recommendations for evaluation of the severity of native valvular regurgitation with two-dimensional and Doppler echocardiography. J Am Soc Echocardiogr 2003;16:777–802.
10 Lang RM, Badano LP, Mor-Avi V, Afilalo J, Armstrong A, Ernande L, Flachskampf FA, Foster E, Goldstein SA, Kuznetsova T, Lancellotti P, Muraru D, Picard MH, Rietzschel ER, Rudski L, Spencer KT, Tsang W, Voigt JU: Recommendations for cardiac chamber quantification by echocardiography in adults: an update from the American Society of Echocardiography and the European Association of Cardiovascular Imaging. Eur Heart J Cardiovasc Imaging 2015;16:233–270.
11 Gaasch WH, Zile MR: Left ventricular structural remodeling in health and disease. J Am Coll Cardiol 2011;58:1733–1740.
12 Falcão-Pires I, Hamdani N, Borbély A, Gavina C, Schalkwijk CG, van der Velden J, van Heerebeek L, Stienen GJ, Niessen HW, Leite-Moreira AF, Paulus WJ: Diabetes mellitus worsens diastolic left ventricular dysfunction in aortic stenosis through altered myocardial structure and cardiomyocyte stiffness. Circulation 2011;124:1151–1159.
13 Borbély A, Falcão-Pires I, van Heerebeek L, Hamdani N, Edes I, Gavina C, Leite-Moreira AF, Bronzwaer JG, Papp Z, van der Velden J, Stienen GJ, Paulus WJ: Hypophosphorylation of the stiff N2B titin isoform raises cardiomyocyte resting tension in failing human myocardium. Circ Res 2009;104:780–786.
14 Russell B, Motlagh D, Ashley WW: Form follows function: how muscle shape is regulated by work. J Appl Physiol 2000;88:1127–1132.
15 Van Heerebeek L, Franssen CP, Hamdani N, Verheugt FW, Somsen GA, Paulus WJ: Molecular and cellular basis for diastolic dysfunction. Curr Heart Fail Rep 2012;9:293–302.
16 Katz AM, Zile MR: New molecular mechanism in diastolic heart failure. Circulation 2006;113:1922–1925.
17 Harvey PA, Leinwand LA: Cellular mechanisms of cardiomyopathy. J Cell Biol 2011;194:355–365.
18 Goffart S, von Kleist-Retzowa JC, Wiesne RJ: Regulation of mitochondrial proliferation in the heart: power-plant failure contributes to cardiac failure in hypertrophy. Cardiovasc Res 2004;64:198–207.
19 Huss JM, Kelly DP: Mitochondrial energy metabolism in heart failure: a question of balance. J Clin Invest 2005;115:547–555.
20 Neubauer S: The failing heart – an engine out of fuel. N Engl J Med 2007;356:1140–1151.
21 Brunk UT, Terman A: Lipofuscin: mechanisms of age-related accumulation and influence on cell function. Free Radic Biol Med 2002;33:611–619.
22 Palmiter KA, Tyska MJ, Dupuis DE, Alpert NR, Warshaw DM: Kinetic differences at the single molecule level account for the functional diversity of rabbit cardiac myosin isoforms. J Physiol 1999;519:6696–6678.
23 Herron TJ, McDonald KS: Small amounts of alpha-myosin heavy chain isoform expression significantly increase power output of rat cardiac myocyte fragments. Circ Res 2002;90:1150–1152.
24 Borisov AB, Raeker MO, Kontrogianni-Konstantopoulos A, Yang K, Kurnit DM, Bloch RJ, Russell MW: Rapid response of cardiac obscurin gene cluster to aortic stenosis: differential activation of Rho-GEF and MLCK and involvement in hypertrophic growth. Biochem Biophys Res Commun 2003;310:910–918.
25 Linke WA: Sense and stretchability: the role of titin and titin-associated proteins in myocardial stress-sensing and mechanical dysfunction. Cardiovasc Res 2008;77:637–648.